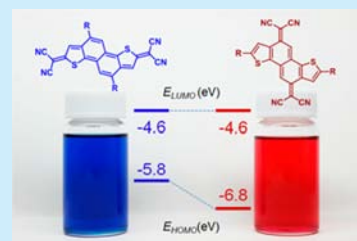


Quinoidal Naphtho[1,2-*b*:5,6-*b'*]dithiophenes for Solution-Processed n-Channel Organic Field-Effect TransistorsTakamichi Mori,<sup>†,‡,§</sup> Naoyuki Yanai,<sup>‡,§</sup> Itaru Osaka,<sup>†</sup> and Kazuo Takimiya<sup>†,‡,\*</sup><sup>†</sup>Emergent Molecular Function Research Group, RIKEN Center for Emergent Matter Science (CEMS), Wako, Saitama 351-0198, Japan<sup>‡</sup>Department of Applied Chemistry, Graduate School of Engineering, Hiroshima University, Higashi-Hiroshima 739-8527, Japan

## S Supporting Information

**ABSTRACT:** A series of new quinoidal naphthodithiophenes, 2,7-bis( $\alpha,\alpha$ -dicyanomethylene)-2,7-dihydronaphtho[1,2-*b*:5,6-*b'*]dithiophenes, in which all the four fused aromatic rings are incorporated into the quinoidal system, were synthesized and evaluated as an n-channel organic semiconductor. Solution-processed field-effect transistors exhibited typical n-channel transistor characteristics with the mobility as high as  $0.1 \text{ cm}^2 \text{ V}^{-1} \text{ s}^{-1}$ , which is higher by more than 1 order of magnitude than those reported for isomeric quinoidal naphthodithiophenes having a naphthoquinoidal structure.



7,7,8,8-Tetracyanoquinodimethane (TCNQ) and its related compounds have been extensively studied not only as superior electron acceptors in charge-transfer (CT) salts<sup>1</sup> but also as p-dopant,<sup>2</sup> diradicals,<sup>3</sup> nonlinear optical materials,<sup>4</sup> and multiphotonic materials.<sup>5</sup> Because of their low-lying LUMO energy levels ( $<4.0 \text{ eV}$  below the vacuum level depending on the molecular structure and the substituent attached), the TCNQ-type materials have recently been focused on as n-channel organic semiconductors.<sup>6</sup> Thiophene analogues of TCNQ (**1**), dicyanomethylene-substituted thienoquinoidals intensively investigated in the 1980s as an electron acceptor for developing highly conductive CT salts,<sup>7</sup> have recently been found to be a promising material class for n-channel organic field-effect transistors (OFETs);<sup>8</sup> in particular, terthienoquinoidal derivatives (**2**) have been reported to afford OFETs showing electron mobilities higher than  $0.1 \text{ cm}^2 \text{ V}^{-1} \text{ s}^{-1}$ .<sup>8c,f</sup> Further molecular explorations on thienoquinoidals with different  $\pi$ -conjugated units such as diketopyrrolopyrrole<sup>9</sup> or thieno[3,2-*b*]thiophene,<sup>10</sup> and thienoacene cores<sup>11</sup> have afforded impressively improved performances on their OFETs with electron mobility of up to  $0.9 \text{ cm}^2 \text{ V}^{-1} \text{ s}^{-1}$ .

From the overview of these recent results on thienoquinoidal-based n-channel organic semiconductors, two important strategies for designing better materials can be deduced. One is to employ extended  $\pi$ -conjugation system that can facilitate better intermolecular  $\pi$ - $\pi$  interaction in the solid state. The other is to introduce alkyl groups to ensure solubility in ordinary organic solvents and to assist molecular ordering in the thin-film state. Considering these strategies, we have recently reported on the synthesis and characterization of naphtho[1,2-*b*:5,6-*b'*]dithiophene (NDT)-based quinoidal molecules ( $\alpha$ -DTTNAPs, Figure 1),<sup>12</sup> where only the naphthalene moiety is incorporated into the quinoidal strand, as a potential material for n-channel organic semiconductors. To explore further possibility of  $\pi$ -extended quinoidal molecules based on

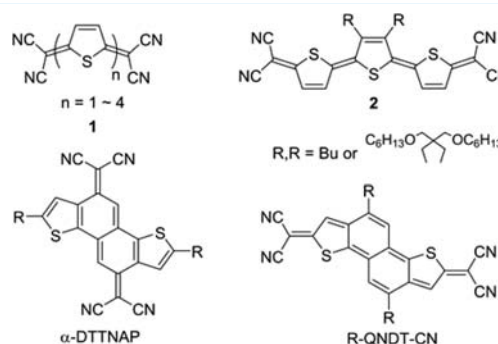


**Figure 1.** Molecular structure of oligothienoquinoidal (**1** and **2**) and NDT-based quinoidal molecules.

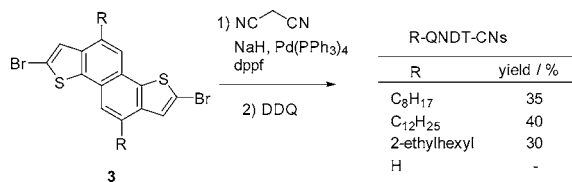
the tetracyclic NDT core, we have synthesized new quinoidal NDTs, namely, 2,7-bis( $\alpha,\alpha$ -dicyanomethylene)-2,7-dihydronaphtho[1,2-*b*:5,6-*b'*]dithiophene (QNDT-CN), where all four fused aromatic rings are incorporated into the quinoidal moiety (Figure 1). We here describe the synthesis, structure, properties, and OFET characteristics of a series of R-QNDT-CN.

The syntheses of QNDT-CN are depicted in Scheme 1, where the palladium-catalyzed Takahashi reaction<sup>13</sup> using the 2,7-dibromo-5,10-dialkyl-NDTs (**3**)<sup>14</sup> as the substrate was employed as the key step, similar to the syntheses of other thienoquinoidal molecules reported.<sup>7-11</sup> In fact, the reactions can afford desired QNDT-CN in moderate yields, except for the nonalkylated parent compound ( $R = \text{H}$ ): although the introduction of dicyanomethyl moieties on the NDT core proceeded, poor solubility of unsubstituted QNDT-CN prevented its isolation in pure form. Other derivatives with

Received: January 7, 2014

Published: February 24, 2014

## Scheme 1. Synthesis of QNDT-CN Derivatives



alkyl groups on the NDT moiety, on the other hand, were able to be isolated and characterized by spectroscopic and combustion elemental analysis. <sup>1</sup>H NMR spectra of QNDT-CNs showed clear two singlets at ca. 7.6 and 7.0 ppm assignable to the two protons on the NDT core. Further structural confirmation was made by single-crystal X-ray analysis of C<sub>12</sub>-QNDT-CN. As demonstrated in Figure 2, C<sub>12</sub>-QNDT-CN molecule consists of the almost planar NDT part with bond length alternation consistent with the canonical thienoquinoidal form.

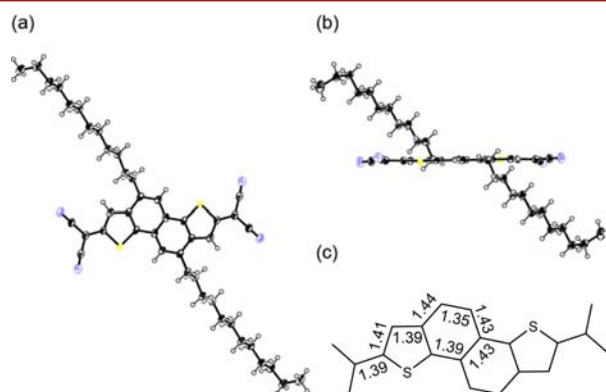


**Figure 2.** Molecular structure of C<sub>12</sub>-QNDT-CN: ORTEP representation. Top view (a) and side view (b), and (c) selected bond lengths (Å) in the thienoquinoidal moiety.

As expected from the extended quinoidal structure over the whole NDT unit, QNDT-CNs have intensive absorption band centered at 630 nm. It should be noted that the absorption bands of QNDT-CNs are significantly red-shifted by ca. 100 nm compared to that of  $\alpha$ -DTTNAPs,<sup>12</sup> the isomeric naphthoquinoidal compounds based on the NDT core (Figure 3a). Similar absorption spectra were obtained for solution-deposited thin films (Supporting Information Figure S3). Cyclic voltammograms of QNDT-CNs (Figure 3b) show one irreversible oxidation and two reversible reduction waves in the typical electrochemical window (−2.0 to +2.0 V vs Ag/AgCl),

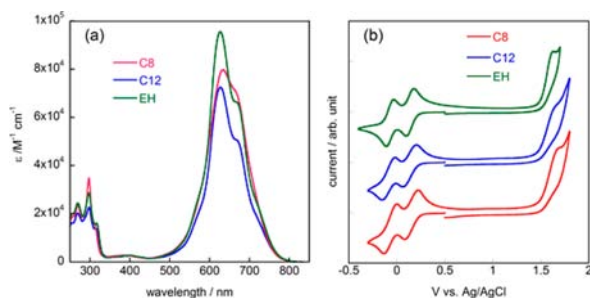


**Figure 3.** UV-vis absorption spectra (a) and cyclic voltammograms (b) of QNDT-CNs.

indicating that the compounds are of ampholytic nature. The electrochemically expected HOMO energy level ( $E_{\text{HOMO}}$ ) and LUMO energy levels ( $E_{\text{LUMO}}$ ) are 5.8 and 4.6 eV below the vacuum level, respectively (Figure 4). The  $E_{\text{LUMO}}$  values of

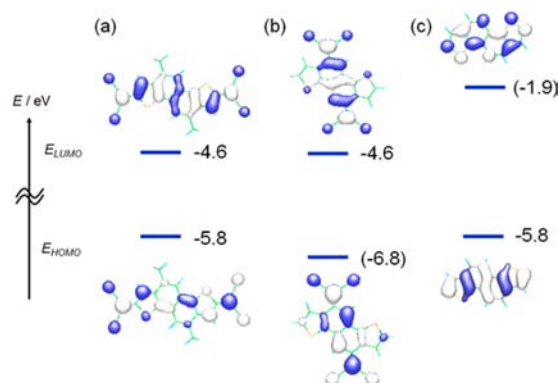


**Figure 4.** Energy diagram of QNDT-CN (a),  $\alpha$ -DTTNAP (b), and parent NDT (c) based on electrochemical data. The  $E_{\text{HOMO}}$  and  $E_{\text{LUMO}}$  in parentheses are estimated from the electrochemical  $E_{\text{LUMO}}$  ( $E_{\text{HOMO}}$ ) and optical  $E_g$ . The spatial distribution of HOMO and LUMO are calculated by the DFT methods at the B3LYP/6-31g(d) level.

QNDT-CNs are almost the same with those of  $\alpha$ -DTTNAPs (4.6 eV below the vacuum level),<sup>12</sup> which could be explained as follows; the QNDT-CN framework has a more extended quinoidal strand than the  $\alpha$ -DTTNAP has, which can stabilize its LUMO (downward shift of  $E_{\text{LUMO}}$ ), whereas incorporation of thiophene ring(s) into the quinoidal strand tends to shift  $E_{\text{LUMO}}$  values upward owing to electron-rich nature of the thiophene rings.<sup>8</sup> These two opposite effects on the thienoquinoidal NDT core could result in almost the same  $E_{\text{LUMO}}$  values of  $\alpha$ -DTTNAPs and QNDT-CNs.

On the other hand, the  $E_{\text{HOMO}}$  values of QNDT-CNs are markedly higher than that of  $\alpha$ -DTTNAPs<sup>12</sup> (6.8 eV below the vacuum level, estimated from electrochemical  $E_{\text{LUMO}}$  and optical  $E_g$ ) and rather close to that of the parent NDT (5.8 eV below the vacuum level), indicating that the present quinoidal naphthodithiophene can be a potential structure for ambipolar organic semiconductors.<sup>8c,g-1</sup> Overall, these differences in the electronic structure between QNDT-CNs and  $\alpha$ -DTTNAPs can be attributed to their spatial distribution of HOMO and LUMO (Figure 4). In the latter system, contribution from the tetracyanonaphthoquinodimethane (TNAP) moiety is quite large on the HOMO and LUMO, whereas contribution from the thiophenes is marginal, even its fused structure. As a result, the compound can be regarded as a “thiophene-fused TNAP derivative”. On the contrary, since HOMO and LUMO of QNDT-CN spread over all four fused aromatic rings, similar to  $\pi$ -extended quinoidals compounds, such as terthienoquinoidals, the  $E_{\text{HOMO}}$  values are effectively elevated.

Due to the long or branched alkyl groups introduced on the naphthalene moiety, solubilities of QNDT-CNs are higher than 3 g L<sup>−1</sup> in chloroform at rt, which is sufficient for the deposition of the thin films by solution processes. In fact, spin-coating from the chloroform solution afforded thin films on glass substrates, which can be utilized as the active layer in OFET devices with a top-gate, bottom-contact configuration using CYTOP films spin-coated on top of the organic layer as the gate dielectric. Demonstrated in Figure 5 are transfer and

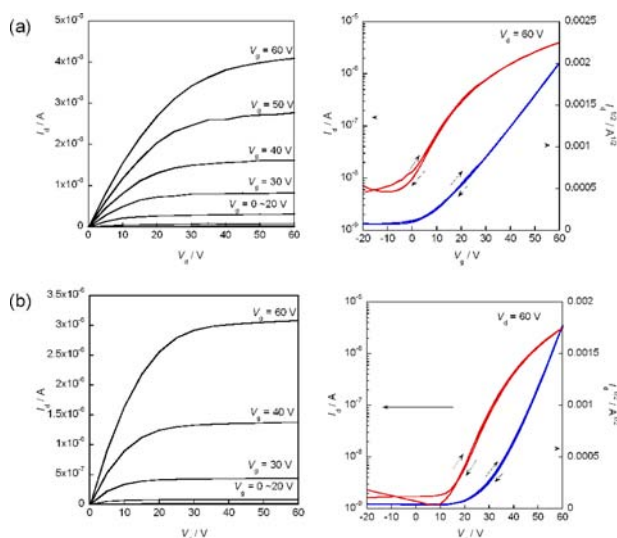


**Figure 5.** Output (left) and transfer (right) characteristics of  $C_{12}$ - (a) and EH-QNDT-CN-based OFETs ( $L = 100 \mu\text{m}$ ,  $W = 3000 \mu\text{m}$ ). (b) Thin films were annealed at  $150^\circ\text{C}$  before the fabrication of CYTOP dielectric.

output curves of the  $C_{12}$ - and EH-QNDT-CN-based devices. As expected from their low-lying  $E_{\text{LUMO}}$ s, typical n-channel behaviors were observed. The extracted mobilities are in the order of  $10^{-2} \text{ cm}^2 \text{ V}^{-1} \text{ s}^{-1}$  (Table S1), which is higher by 1 order of magnitude than those for  $\alpha$ -DTTNAPs, the isomeric naphthoquinoidal counterparts. We also examined the QNDT-CN-based devices under the negative bias, but no clear p-channel operation was observed. This could be attributed to the fact that their  $E_{\text{HOMO}}$  values are still too low to cause hole injection from the source electrode.

Thermal annealing of the thin films improved the device characteristics, though it was not very significant. This could be explained by the fact that the crystallinity of thin films was only slightly improved by annealing (at 50, 100, and  $150^\circ\text{C}$  for 30 min), as indicated by the XRD patterns of the thin films (Figure 6 and Figure S4). In fact, only the first- ( $C_8$ -QNDT-CN, EH-QNDT-CN) or up to the second-order peaks ( $C_{12}$ -QNDT-CN) were observed. In addition, extracted  $d$ -spacings can be related to the length of the alkyl groups:  $C_8$  derivative,  $15.5 \text{ \AA}$ ;  $C_{12}$  derivative,  $19.5 \text{ \AA}$ ; and EH derivative,  $13.2 \text{ \AA}$ . The XRD pattern of  $C_{12}$ -QNDT-CN cannot be indexed by the single-crystal unit cell, indicating that the packing structure in the thin-film state is different from that in the bulk single crystal.<sup>15</sup> Considering the length of the quinoidal core (ca.  $15 \text{ \AA}$ ) extracted from the single-crystal structure analysis of  $C_{12}$ -QNDT-CN and the  $d$ -spacings in the thin films dependent on the length of the alkyl groups, the molecular orientation in the crystalline domains could be edge-on with the alkyl groups standing on the substrate.

It should be emphasized that the EH-QNDT-CN-based devices afforded the highest mobility among the devices based on the present materials, even though the crystallinity was lower as judged from the XRD patterns: the maximum mobility higher than  $0.1 \text{ cm}^2 \text{ V}^{-1} \text{ s}^{-1}$  was obtained after annealing of the thin film at  $150^\circ\text{C}$ . The higher mobility of the EH-QNDT-CN-based devices than those of  $C_8$ - or  $C_{12}$ -QNDT-CN could be explained by the uniformity of the thin films. Figure 6 also shows AFM images of the spin-coated thin films of  $C_{12}$ - and EH-QNDT-CN on the glass substrates (right). The surface

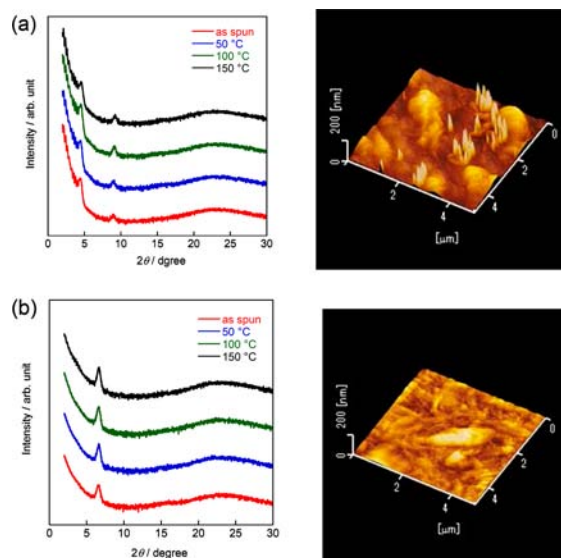


**Figure 6.** Left: X-ray diffraction (XRD) patterns of spin-coated thin films of  $C_{12}$ - (a) and EH-QNDT-CN on the glass substrate (b). Right: AFM images of spin coated thin films of  $C_{12}$ - (a) and EH-QNDT-CN (b) annealed at  $150^\circ\text{C}$ .

roughness (rms) of  $C_8$ - (Figure S1) and  $C_{12}$ -QNDT-CN is 11.5 and  $19.5 \text{ nm}$ , respectively, whereas that for EH-QNDT-CN is less than  $5.0 \text{ nm}$ . For the top-gate devices, the surface of thin film acts as the channel region, and thus uniformity of thin film with smaller surface roughness should be desirable. As a result, although its crystallinity can be relatively low, higher uniformity and rather flat surface of the EH-QNDT-CN thin film is quite beneficial to achieve better performance in the FET devices.

In summary, we have successfully synthesized a series of alkyl-substituted QNDT-CNs, thienoquinoidal NDTs with dicyanomethylene termini, and elucidated their electronic structures and thin-film transistor properties. The characteristic features of QNDT-CNs are (1) low-lying  $E_{\text{LUMO}}$  ( $4.6 \text{ eV}$  below the vacuum level) suitable for n-channel operation; (2) relatively high-lying  $E_{\text{HOMO}}$ , which is quite different from the isomeric  $\alpha$ -DTTNAPs; (3) good solubility in common organic solvents, allowing deposition of thin films from the solution; (4) moderately high electron mobility ( $\sim 0.1 \text{ cm}^2 \text{ V}^{-1} \text{ s}^{-1}$ ) observed for solution-processed, top-gate, bottom-contact devices. These results indicate that the thienoquinoidal NDT framework is another potential molecular structure for the development of n-channel organic semiconductors. Not just low-lying  $E_{\text{LUMO}}$  values but relatively high-lying  $E_{\text{HOMO}}$  values of QNDT-CN could be an additional attractive feature for further development of new  $\pi$ -conjugated systems. Thus, molecule modification on the thienoquinoidal NDT core for developing not only n-channel but also ambipolar organic semiconductors is now underway in our group.

## ■ ASSOCIATED CONTENT

### § Supporting Information

Experimental details, instrumentation, NMR spectra, CIF for  $C_{12}$ -QNDT-CN. This material is available free of charge via the Internet at <http://pubs.acs.org>.

## ■ AUTHOR INFORMATION

## Corresponding Author

\*E-mail: takimiya@riken.jp.

## Author Contributions

<sup>§</sup>T.M. and N.Y. contributed equally to this work.

## Notes

The authors declare no competing financial interest.

## ■ ACKNOWLEDGMENTS

This work was financially supported by Grants-in-Aid for Scientific Research (No. 23245041) from MEXT, Japan. HRMS was measured at the Natural Science Center for Basic Research and Development (N-BARD), Hiroshima University, and at the Materials Characterization Support Unit in RIKEN Advanced Technology Support Division.

## ■ REFERENCES

- (1) (a) Ferraris, J.; Cowan, D. O.; Walatka, V.; Perlstein, J. H. *J. Am. Chem. Soc.* **1973**, *95*, 948–949. (b) Martin, N.; Segura, J. L.; Seoane, C. *J. Mater. Chem.* **1997**, *7*, 1661–1676.
- (2) Soeda, J.; Hirose, Y.; Yamagishi, M.; Nakao, A.; Uemura, T.; Nakayama, K.; Uno, M.; Nakazawa, Y.; Takimiya, K.; Takeya, J. *Adv. Mater.* **2011**, *23*, 3309–3314.
- (3) (a) Abe, M. *Chem. Rev.* **2013**, *113*, 7011–7088. (b) Ortiz, R. P.; Casado, J.; Hernández, V.; Navarrete, L.; Viruela, P. M.; Ortí, E.; Takimiya, K.; Otsubo, T. *Angew. Chem., Int. Ed.* **2007**, *46*, 9057–9061.
- (4) (a) Higuchi, H.; Nakayama, T.; Koyama, H.; Ojima, J.; Wada, T.; Sasabe, H. *Bull. Chem. Soc. Jpn.* **1995**, *68*, 2363–2377. (b) Kishi, R.; Dennis, M.; Fukuda, K.; Murata, Y.; Morita, K.; Uenaka, H.; Nakano, M. *J. Phys. Chem. C* **2013**, *117*, 21498–21508.
- (5) Raymond, J. E.; Casado, J.; Lopez Navarrete, J. T.; Takimiya, K.; Goodson, T. *J. Phys. Chem. Lett.* **2011**, *2*, 2179–2183.
- (6) (a) Brown, A. R.; de Leeuw, D. M.; Lous, E. J.; Havinga, E. E. *Synth. Met.* **1994**, *66*, 257–261. (b) Laquindanum, J. G.; Katz, H. E.; Dodabalapur, A.; Lovinger, A. J. *J. Am. Chem. Soc.* **1996**, *118*, 11331–11332. (c) de Leeuw, D. M.; Simenon, M. M. J.; Brown, A. R.; Einerhand, R. E. F. *Synth. Met.* **1997**, *87*, 53–59. (d) Menard, E.; Podzorov, V.; Hur, S. H.; Gaur, A.; Gershenson, M. E.; Rogers, J. A. *Adv. Mater.* **2004**, *16*, 2097–2101.
- (7) (a) Casado, J.; Ponce Ortiz, R.; Lopez Navarrete, J. T. *Chem. Soc. Rev.* **2012**, *41*, 5672–5686. (b) Gronowitz, S.; Uppström, B. *Acta Chem. Scand., B* **1974**, *28*, 981–985. (c) Yui, K.; Aso, Y.; Otsubo, T.; Ogura, F. *J. Chem. Soc., Chem. Commun.* **1987**, 1816–1817. (d) Yui, K.; Ishida, H.; Aso, Y.; Otsubo, T.; Ogura, F. *Chem. Lett.* **1987**, 2339–2342. (e) Yui, K.; Aso, Y.; Otsubo, T.; Ogura, F. *Bull. Chem. Soc. Jpn.* **1989**, *62*, 1539–1546. (f) Yui, K.; Ishida, H.; Aso, Y.; Otsubo, T.; Ogura, F.; Kawamoto, A.; Tanaka, J. *Bull. Chem. Soc. Jpn.* **1989**, *62*, 1547–1555.
- (8) (a) Pappenfus, T. M.; Chesterfield, R. J.; Frisbie, C. D.; Mann, K. R.; Casado, J.; Raff, J. D.; Miller, L. L. *J. Am. Chem. Soc.* **2002**, *124*, 4184–4185. (b) Casado, J.; Miller, L. L.; Mann, K. R.; Pappenfus, T. M.; Higuchi, H.; Ortí, E.; Milian, B.; Pou-Amerigo, R.; Hernandez, V.; Lopez Navarrete, J. T. *J. Am. Chem. Soc.* **2002**, *124*, 12380–12388. (c) Chesterfield, R. J.; Newman, C. R.; Pappenfus, T. M.; Ewbank, P. C.; Haukaas, M. H.; Mann, K. R.; Miller, L. L.; Frisbie, C. D. *Adv. Mater.* **2003**, *15*, 1278–1282. (d) Berlin, A.; Grimoldi, S.; Zotti, G.; Osuna, R. M.; Ruiz Delgado, M. C.; Ortiz, R. P.; Casado, J.; Hernandez, V.; Lopez Navarrete, J. T. *J. Phys. Chem. B* **2005**, *109*, 22308–22318. (e) Kunugi, Y.; Takimiya, K.; Toyoshima, Y.; Yamashita, K.; Aso, Y.; Otsubo, T. *J. Mater. Chem.* **2004**, *14*, 1367–1369. (f) Handa, S.; Miyazaki, E.; Takimiya, K.; Kunugi, Y. *J. Am. Chem. Soc.* **2007**, *129*, 11684–11685. (g) Handa, S.; Miyazaki, E.; Takimiya, K. *Chem. Commun.* **2009**, 3919–3921. (h) Ribierre, J. C.; Fujihara, T.; Watanabe, S.; Matsumoto, M.; Muto, T.; Nakao, A.; Aoyama, T. *Adv. Mater.* **2010**, *22*, 1722–1726. (i) Suzuki, Y.; Miyazaki, E.; Takimiya, K. *J. Am. Chem. Soc.* **2010**, *132*, 10453–10466. (j) Suzuki, Y.; Shimawaki, M.; Miyazaki, E.; Osaka, I.; Takimiya, K. *Chem. Mater.* **2011**, *23*, 795–804. (k) Ribierre, J. C.; Watanabe, S.; Matsumoto, M.; Muto, T.; Hashizume, D.; Aoyama, T. *J. Phys. Chem. C* **2011**, *115*, 20703–20709.
- (9) (a) Zhong, H.; Smith, J.; Rossbauer, S.; White, A. J. P.; Anthopoulos, T. D.; Heeney, M. *Adv. Mater.* **2012**, *24*, 3205–3211. (b) Qiao, Y.; Guo, Y.; Yu, C.; Zhang, F.; Xu, W.; Liu, Y.; Zhu, D. *J. Am. Chem. Soc.* **2012**, *134*, 4084–4087.
- (10) Wu, Q.; Ren, S.; Wang, M.; Qiao, X.; Li, H.; Gao, X.; Yang, X.; Zhu, D. *Adv. Funct. Mater.* **2013**, *23*, 2277–2284.
- (11) (a) Kashiki, T.; Miyazaki, E.; Takimiya, K. *Chem. Lett.* **2009**, *38*, 568–569. (b) Wu, Q.; Li, R.; Hong, W.; Li, H.; Gao, X.; Zhu, D. *Chem. Mater.* **2011**, *23*, 3138–3140.
- (12) Yanai, N.; Mori, T.; Shinamura, S.; Osaka, I.; Takimiya, K. *Org. Lett.* **2014**, *16*, 240–243.
- (13) Uno, M.; Seto, K.; Takahashi, S. *J. Chem. Soc., Chem. Commun.* **1984**, 932–933.
- (14) (a) Shinamura, S.; Sugimoto, R.; Yanai, N.; Takemura, N.; Kashiki, T.; Osaka, I.; Miyazaki, E.; Takimiya, K. *Org. Lett.* **2012**, *14*, 4718–4721. (b) Osaka, I.; Kakara, T.; Takemura, N.; Koganezawa, T.; Takimiya, K. *J. Am. Chem. Soc.* **2013**, *135*, 8834–8837.
- (15) See Supporting Information for simulated powder pattern of C12-QNDT-CN.